Betulinic Acid Triggers CD95 (APO-1/Fas)- and p53-independent Apoptosis via Activation of Caspases in Neuroectodermal Tumors[1]

Simone Fulda, Claudia Friesen, Marek Los, Carsten Scaffidi, Walter Mier, Mary Benedict, Gabriel Nuñez, Peter H. Krammer, Marcus E. Peter, and Klaus-Michael Debatin[2]

Division of Hematology/Oncology, University Children's Hospital and Division of Molecular Oncology, German Cancer Research Center, D-69120 Heidelberg, Germany [S. F., C. F., M. L., K-M. D.]; Divisions of Immunogenetics [C. S., P. H. K., M. E. P.] and Molecular Toxicology [W. M.], German Cancer Research Center, D-69120 Heidelberg, Germany; and Department of Pathology, University of Michigan Medical School, Ann Arbor, Michigan 48109 [M. B., G. N.]

ABSTRACT

Betulinic acid (BA), a melanoma-specific cytotoxic agent, induced apoptosis in neuroectodermal tumors, such as neuroblastoma, medulloblastoma, and Ewing's sarcoma, representing the most common solid tumors of childhood. BA triggered an apoptosis pathway different from the one previously identified for standard chemotherapeutic drugs. BA-induced apoptosis was independent of CD95-ligand/receptor interaction and accumulation of wild-type p53 protein, but it critically depended on activation of caspases (interleukin 1β-converting enzyme/Ced-3-like proteases). FLICE/MACH (caspase-8), considered to be an upstream protease in the caspase cascade, and the downstream caspase CPP32/YAMA/Apopain (caspase-3) were activated, resulting in cleavage of the prototype substrate of caspases PARP. The broad-spectrum peptide inhibitor benzyloxycarbonyl-Val-Ala-Asp-fluoromethylketone, which blocked cleavage of FLICE and PARP, also completely abrogated BA-triggered apoptosis. Cleavage of caspases was preceded by disturbance of mitochondrial membrane potential and by generation of reactive oxygen species. Overexpression of Bcl-2 and Bcl-x_L conferred resistance to BA at the level of mitochondrial dysfunction, protease activation, and nuclear fragmentation. This suggested that mitochondrial alterations were involved in BA-induced activation of caspases. Furthermore, Bax and Bcl-x_s, two death-promoting proteins of the Bcl-2 family, were up-regulated following BA treatment. Most importantly, neuroblastoma cells resistant to CD95- and doxorubicin-mediated apoptosis were sensitive to treatment with BA, suggesting that BA may bypass some forms of drug resistance. Because BA exhibited significant antitumor activity on patients' derived neuroblastoma cells *ex vivo*, BA may be a promising new agent for the treatment of neuroectodermal tumors *in vivo*.

INTRODUCTION

Cytotoxic drugs, irrespective of their intracellular target, have been shown to cause death of sensitive target cells by inducing apoptosis (1). We previously identified the CD95 (APO-1/Fas) system as a key mediator of drug-induced apoptosis in leukemia and neuroblastoma cells (2, 3). Upon treatment with cytotoxic drugs, CD95-L[3] was induced and caused apoptosis in an autocrine or paracrine manner (2, 3). CD95 is a cell surface receptor of the TNF/nerve growth factor receptor superfamily expressed on a variety of normal and neoplastic cells (4–7). Cross-linking of CD95 by either the natural ligand or an agonistic antibody rapidly induces apoptosis in sensitive cells by activating a death signaling cascade (8). FADD/MORT-1 binds to the

death domains of oligomerized CD95 receptors to form the DISC (8). FLICE/MACH (caspase-8), a recently cloned new member of the family of caspases (interleukin 1β-converting enzyme/Ced-3-like proteases) and considered to be the most upstream component of the caspase cascade (9–12), is activated upon recruitment to the DISC during death receptor-triggered apoptosis and catalyzes cleavage of downstream members of the caspase family, leading to proteolysis of substrates, such as the nuclear enzyme PARP (12–14). CD95-L is a M_r 40,000 type II transmembrane molecule of the TNF/nerve growth factor family of ligands (15) that may also occur in a soluble form released after proteolytic cleavage from the cell surface (16).

Several recent reports have implied that mitochondria may play a major role in the apoptotic process (17–19). A crucial, common step in apoptosis is postulated to involve loss of mitochondrial membrane potential through opening of permeability transition pores, resulting in hyperproduction of ROS (17). The Bcl-2 family of proteins is composed of several members that play a key role in regulation of apoptosis through homo- or heterodimerization (20). Bcl-2 and most of its homologues have been localized to intracellular membranes, including the mitochondrial membrane (17). Overexpression of Bcl-2 has been shown to inhibit opening of mitochondrial permeability transition pores, which are thought to account for ΔΨ$_m$ collapse in preapoptotic cells (18). Recent data indicate that Bcl-x_L and Bcl-2 have pore-forming properties in lipid membranes, suggesting that Bcl-2 family members may participate in regulation of molecule fluxes across the mitochondrial membrane (21, 22).

Apoptosis pathways may be disrupted in tumor cells, conferring a survival advantage (6). For solid tumors of childhood, chemotherapy is an important treatment modality (23). Although many tumors initially respond to chemotherapy, the prognosis for children who relapse or present with disseminated disease remains poor. Therefore, insight into the molecular mechanisms that regulate apoptosis in tumor cells and identification of new cytotoxic agents that enhance or restore the ability of tumor cells to undergo apoptosis may be crucial for more effective therapies. BA, a pentacyclic triterpene prepared from the bark of white birch trees, has recently been identified as a new melanoma-specific cytotoxic compound that induced apoptotic death in target cells (24). However, the molecular pathways involved in BA-mediated apoptosis have not been defined thus far. Because we found that BA efficiently induced apoptosis in neuroectodermal tumor cells, we analyzed the molecular requirements for BA-induced cell death and found that they differed from the mechanism of action recently identified for conventional cytotoxic drugs.

MATERIALS AND METHODS

Drugs. BA (Aldrich, Steinheim, Germany) and Doxo (Farmitalia, Milan, Italy) were provided as pure substances and dissolved in DMSO (4 mg/ml BA) or sterile water (1 mg/ml Doxo) before each experiment.

Cell Culture. Neuroblastoma (SH-EP, IMR-32, Kelly, and LAN-5; kindly provided by Professor M. Schwab, German Cancer Research Center, Heidelberg, Germany), medulloblastoma (Daoy; kindly provided by Dr. T. Pietsch, Department of Neuropathology, University of Bonn Medical Center, Bonn,
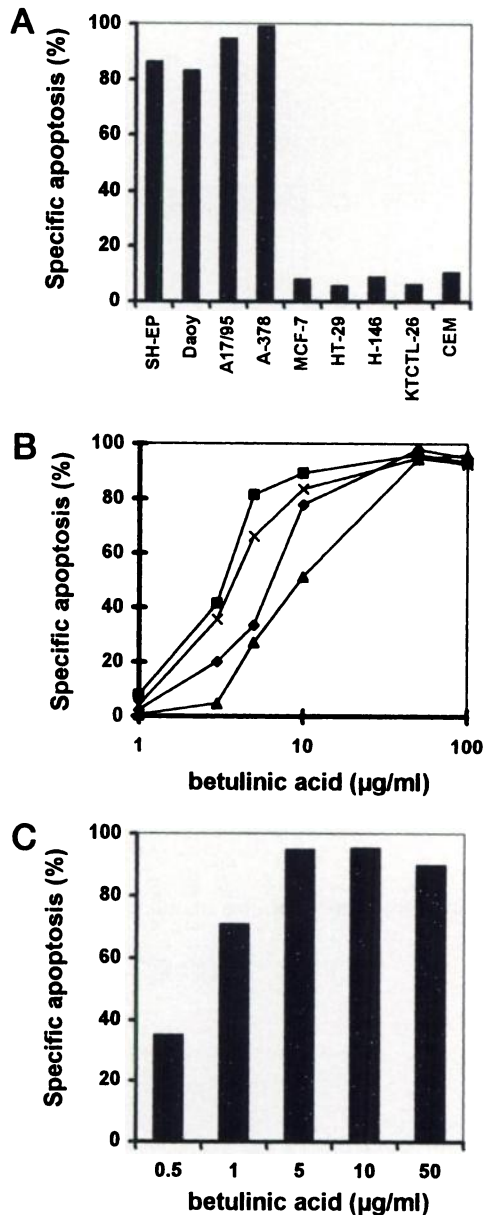
Fig. 1. Induction of apoptosis by BA. *A*, induction of apoptosis by BA in various tumor cell lines. Cells were treated with 10 μg/ml BA for 72 h. Apoptosis was assessed by FACS analysis of propidium iodide-stained nuclei. Percentage of specific apoptosis was calculated as follows: [experimental apoptosis (%) − spontaneous apoptosis in medium (%)]/[100% − spontaneous apoptosis in medium (%)] × 100. Cell lines tested were neuroblastoma (*SH-EP*), medulloblastoma (*Daoy*), Ewing's sarcoma (*A17/95*), melanoma (*A-378*), breast carcinoma (*MCF-7*), colon carcinoma (*HT-29*), small cell lung carcinoma (*H-146*), renal cell carcinoma (*KTCTL-26*), and T-cell leukemia (*CEM*). *Columns*, mean of triplicates; SDs were less than 10%. Similar results were obtained in three separate experiments. *B*, dose response of BA-induced apoptosis. SH-EP (◆), LAN-5 (▲), IMR-32 (×), and Kelly (■) neuroblastoma cells were treated with BA for 72 h at the indicated concentrations. Apoptosis was assessed by FACS analysis of propidium iodide-stained nuclei. Percentage of specific apoptosis was calculated as described for *A. Data points*, mean of triplicates; SDs were less than 10%. Similar results were obtained in three separate experiments. *C*, dose response of BA-induced apoptosis in neuroblastoma cells *ex vivo*. Single-cell suspensions were prepared from tumor samples obtained from surgical resection prior to chemotherapy and incubated with indicated concentrations of BA for 18 h. Two-color fluorescence staining using FITC-conjugated mouse antihuman GD2 antibody and biotinylated annexin V followed by streptavidin-phycoerythrin was performed on a flow cytometer. Specific apoptosis was calculated as described for *A*. Representative data from one of two patients are shown. Experiments were done in triplicate; SDs were less than 10%.

Germany), Ewing's sarcoma (A17/95; kindly provided by Dr. U. Anderer, Institute of Pathology, Humboldt University, Berlin, Germany), melanoma (A-378), breast carcinoma (MCF-7), colon carcinoma (HT-29), small cell lung carcinoma (H-146), renal cell carcinoma (KTCTL-26; all kindly provided by

H. Lörke, German Cancer Research Center, Heidelberg, Germany), and T-cell leukemia (CEM) cells were cultured in RPMI 1640 (Life Technologies, Inc., Eggenstein, Germany) supplemented with 10% heat-inactivated FCS (Conco, Wiesbaden, Germany), 10 mM HEPES, pH 7.3 (Biochrom, Berlin, Germany), 100 units/ml penicillin (Life Technologies, Inc.), 100 μg/ml streptomycin (Life Technologies, Inc.), and 2 mM L-glutamine (Biochrom). SH-EP neuroblastoma cells stably transfected with bcl-2, bcl-x$_L$, or vector control were cultured in Dulbecco's minimal Eagle's medium (Life Technologies, Inc.) containing 500 μg/ml G418 (Geneticin, Life Technologies, Inc.) as described previously (25, 26). SH-EP^{CD95R} and SH-EP^{DoxoR} cells, variants of SH-EP neuroblastoma cells resistant to anti-CD95 and Doxo, respectively, were generated by continuous culture in the presence of the agonistic anti-APO-1 (anti-CD95) antibody (1 μg/ml; Ref. 27) or Doxo (0.1 μg/ml) for more than 6 months. For experiments, resistant cells were washed and cultured in medium without anti-APO-1 (anti-CD95) for 24 h or without Doxo for 2 weeks.

Determination of Apoptosis. Quantification of DNA fragmentation was performed by FACS analysis of propidium iodide stained nuclei as described previously (28). Cells were analyzed for DNA content by flow cytometry (FACScan, Becton Dickinson, Heidelberg, Germany) using CELLQuest software. Early apoptotic changes were identified by staining with biotinylated annexin V (Bender Med Systems, Vienna, Austria) following the manufacturer's instructions. Annexin V binds to exposed phosphatidylserine on the surface of apoptotic cells (29). Cells were analyzed by flow cytometry (FAC-Scan, Becton Dickinson) using CELLQuest software.

Preparation of Neuroblastoma Tumor Samples. Fresh tumor samples from two patients with neuroblastoma stages IVS and IV, respectively, were obtained from surgical resections prior to chemotherapy and immediately analyzed. Single-cell suspensions were prepared using DNase (0.154 mg/ml), collagenase (0.416 mg/ml), and hyaluronidase (0.33 mg/ml; Boehringer Mannheim). Two-color fluorescence using FITC-conjugated mouse antihuman GD2 antibody (IgG2a, 0.2 mg/ml; kindly provided by R. Handgretinger, University of Tuebingen, Tuebingen, Germany) and biotinylated annexin V (Bender Med Systems) followed by streptavidin-phycoerythrin was performed to detect apoptotic neuroblastoma cells (30).

Incubation with Tripeptide Inhibitor of Caspases or F(ab')$_2$ Anti-APO-1 (anti-CD95) Antibody Fragments. The broad-range tripeptide inhibitor of caspases zVAD-fmk (Enzyme Systems Products, Dublin, CA) was used at a concentration of 60 μM. Preparations of F(ab')$_2$ anti-APO-1 (anti-CD95) antibody fragments and isotype-matched antibody FII23 (IgG3) were performed as described previously (31). Cells were incubated with 10 μg/ml F(ab')$_2$ anti-APO-1 antibody fragments or 10 μg/ml F(ab')$_2$ FII23 antibody fragments for 1 h at 37°C prior to addition of BA.

Determination of Caspase Activity. Caspase activity was measured by FACS analysis as described previously (32). Briefly, cells were loaded in hypotonic medium with the fluorogenic substrate Val-Ala-Asp-[2(4-meth-oxynaphthylamide)] at a final concentration of 50 μM (Enzyme Systems Products). Fluorescence was measured by flow cytometer (FACS Vantage, Becton Dickinson) using an excitation wavelength of 365 nm and an emission wavelength of 425 nm.

Assessment of Mitochondrial Potential, Intracellular Peroxides, and Membrane Peroxidation. The cationic lipophilic fluorochrome DiOC$_6$(3) (460 ng/ml, Molecular Probes, Eugene, OR) was used to measure the ΔΨ$_m$, HE (126 ng/ml, Molecular Probes) was used to determine ROS generation, and NAO (94 ng/ml, Molecular Probes) was used to determine lipid peroxidation (17). Cells were incubated for 12 min at 37°C in the presence of the fluorochromes, washed in PBS/1% FCS, and immediately analyzed by flow cytometry (FACScan, Becton Dickinson). DiOC$_6$(3) and NAO fluorescence were recorded in fluorescence 1; He fluorescence was assessed in fluorescence 3. The percentage of cells with low mitochondrial potential or enhanced ROS production was calculated in comparison to untreated control cells.

RT-PCR for CD95-L mRNA. Total RNA was prepared using the Qiagen total RNA kit (Qiagen, Hilden, Germany). RNA was converted to cDNA by reverse transcription and amplified for 38 cycles by PCR in a thermocycler (Stratagene, Heidelberg, Germany) using the Gene Amplification RNA-PCR kit (Perkin-Elmer, Branchburg, NJ) following the manufacturer's instructions. Primers used for amplification of the CD95-L fragment are according to the sequence of human CD95-L (15, 33). Expression of β-actin (MWG-Biotech, Ebersberg, Germany) was used as an internal standard for RNA integrity and
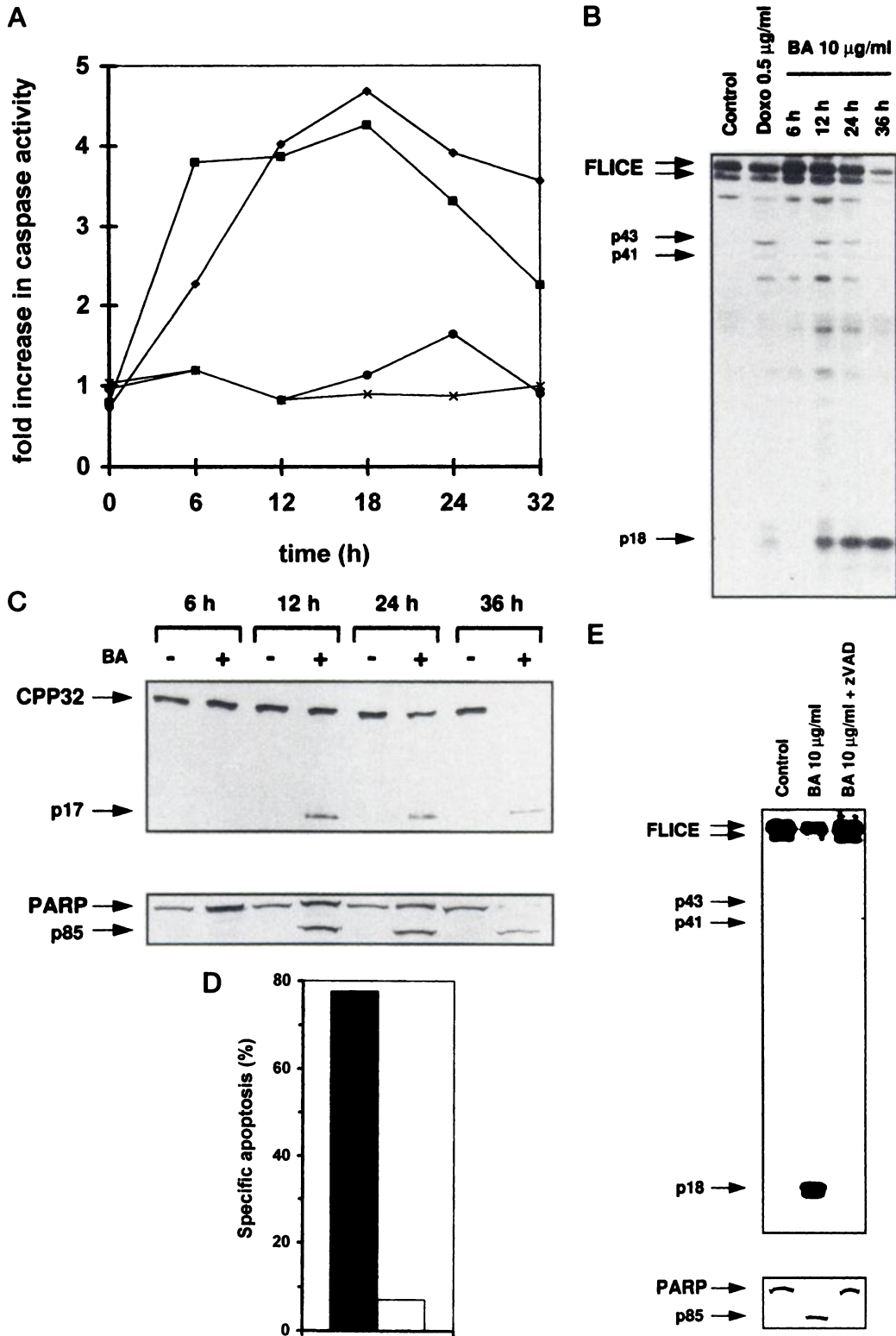
Fig. 2. BA-induced activation of caspases. *A*, analysis of caspase activity. SH-EP neuroblastoma cells were incubated with 1 (×), 5 (●), 10 (♦), and 50 (■) μg/ml BA for the times indicated. Cells were permeabilized by hypotonic shock, incubated with 50 μM of the fluorogenic substrate Val-Ala-Asp-[2(4-methoxynaphthylamide)], and analyzed with a flow cytometer. *Data points*, mean from three independent experiments in triplicate. SDs were less than 10%. *B* and *C*, cleavage of FLICE, CPP32, and PARP. SH-EP neuroblastoma cells were treated with 10 μg/ml BA for indicated times or with 0.5 μg/ml Doxo for 24 h. Forty μg of protein per lane, isolated from cell lysates, were separated by 12% SDS-PAGE. Immunodetection of FLICE (*B*), CPP32 (*C*), and PARP (*C*) proteins was performed by mouse anti-FLICE monoclonal antibody, mouse anti-CPP32 monoclonal antibody, or rabbit anti-PARP polyclonal antibody and ECL. Processing of FLICE, which was detected as a double band corresponding to two FLICE isoforms (caspase-8/a and 8/b),[4] resulted in the p43 and p41 cleavage intermediates derived from caspase-8/a and 8/b, respectively, and the p18 active subunit. *D*, inhibition of BA-induced apoptosis by zVAD-fmk. SH-EP neuroblastoma cells were treated with 10 μg/ml BA for 72 h in the absence (■) or presence (□) of 60 μM zVAD-fmk. Specific apoptosis was determined and calculated as described in the legend to Fig. 1A. *Columns*, mean from three independent experiments in triplicate. SDs were less than 10%. *E*, inhibition of BA-induced cleavage of FLICE and PARP by zVAD-fmk. SH-EP neuroblastoma cells were treated with 10 μg/ml BA for 24 h with or without 60 μM zVAD-fmk. Western blot analysis for FLICE and PARP cleavage was performed as described for *B*.

---

[4] Scaffidi, C., Medema, J. P., Krammer, P. H., and Peter, M. E. FLICE is predominantly expressed as two functionally active isoforms, caspase-8/a and 8/b. J. Biol. Chem., in press.
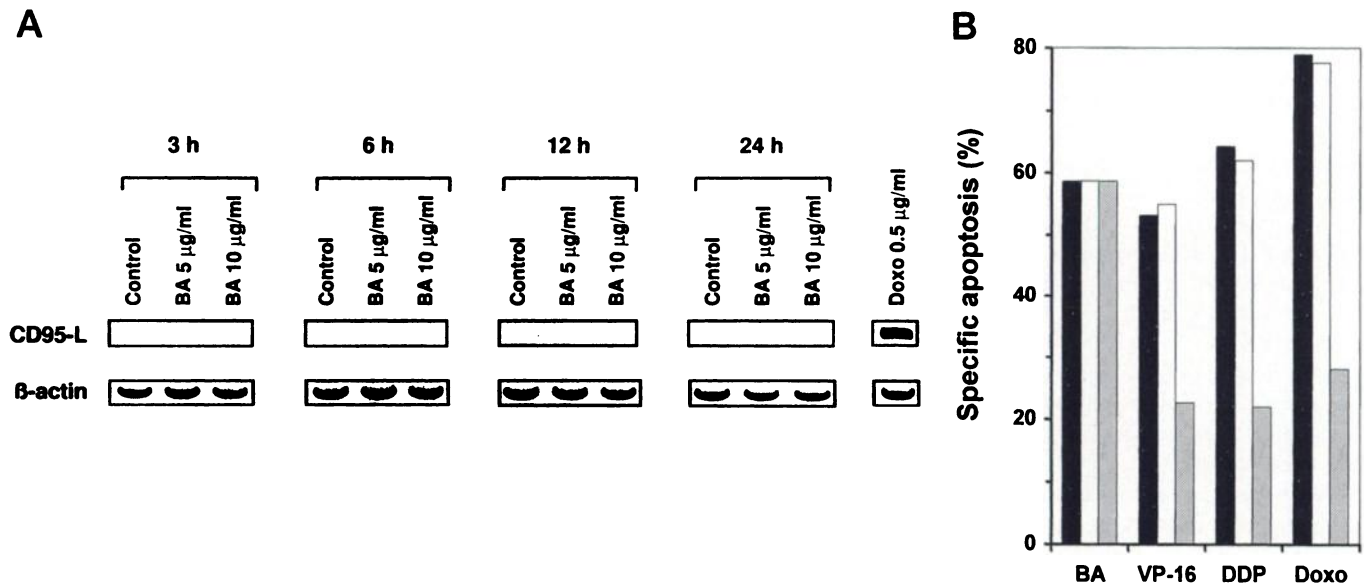
Fig. 3. CD95-independent induction of apoptosis by BA. *A*, analysis of CD95-L mRNA expression by RT-PCR. SH-EP neuroblastoma cells were incubated with 5 and 10 µg/ml BA for the indicated times or with 0.5 µg/ml Doxo for 24 h. CD95-L mRNA expression was determined by RT-PCR. Expression of β-actin was used to control RNA integrity and equal gel loading. *B*, lack of inhibition of BA-induced apoptosis by F(ab')₂ anti-APO-1 (anti-CD95). SH-EP neuroblastoma cells were treated with 10 µg/ml BA, 50 µg/ml VP-16, 10 µg/ml cisplatinum (*DDP*), or 0.5 µg/ml Doxo for 72 h after preincubation for 1 h with medium (■), 10 µg/ml F(ab')₂ FII23 (IgG3 control antibody; □), or 10 µg/ml F(ab')₂ anti-APO-1 (anti-CD95; blocking antibody; ▨). Specific apoptosis was determined and calculated as described in the legend to Fig. 1*A*. *Columns*, mean from three independent experiments in triplicate. SDs were less than 10%.

equal gel loading. PCR products were run at 60 V for 2 h on a 1.5% agarose gel stained with ethidium bromide and visualized by UV illumination.

Western Blot Analysis. Cells were lysed for 30 min at 4°C in PBS with 0.5% Triton X (Serva, Heidelberg, Germany) and 1 mM phenylmethylsulfonyl fluoride (Sigma, Deisenhofen, Germany) followed by high-speed centrifugation. Membrane proteins were eluted in buffer containing 0.1 M glycine, pH 3.0, and 1.5 M Tris, pH 8.8. Protein concentration was assayed using bicinchoninic acid (Pierce Chemical Co., Rockford, IL). Forty µg of protein per lane were separated by 12% SDS-PAGE and electroblotted onto nitrocellulose (Amersham, Braunschweig, Germany). Equal protein loading was controlled by Ponceau red staining of membranes. After blocking for 1 h in PBS supplemented with 2% BSA (Sigma) and 0.1% Tween 20 (Sigma), immunodetection of FLICE, CPP32, PARP, Bax, Bcl-x, Bcl-2, and p53 protein was done using mouse anti-FLICE monoclonal antibody C15 (1:5 dilution of hybridoma supernatant), mouse anti-CPP32 monoclonal antibody (1:1000, Transduction Laboratories, Lexington, KY), rabbit anti-PARP polyclonal antibody (1:10000, Enzyme Systems Products), rabbit anti-Bax polyclonal antibody (1:500, Calbiochem, Bad Soden, Germany), rabbit anti-Bcl-x polyclonal antibody (1:1000, Santa Cruz Biotechnology, Santa Cruz, CA), mouse anti-Bcl-2 monoclonal antibody (1:1000, Santa Cruz Biotechnology), mouse anti-p53 monoclonal antibody (1:1000, Transduction Laboratories), and goat anti-mouse IgG or goat antirabbit IgG (1:5000, Santa Cruz Biotechnology). ECL (Amersham) was used for detection.

RESULTS

BA Induces Apoptosis in Neuroectodermal Cells. We initially screened a panel of tumor cell lines for sensitivity to BA cytotoxicity. Neuroblastoma, medulloblastoma, and Ewing's sarcoma cells were found to be highly responsive to BA, in addition to melanoma cells that had previously been reported to respond to BA (24). In contrast, epithelial tumors, such as breast carcinoma, colon carcinoma, small cell lung carcinoma, and renal cell carcinoma, as well as T-cell leukemia cells, were almost completely refractory to treatment with BA (Fig. 1*A*). We then selected neuroblastoma as a prototype chemosensitive tumor to explore the molecular requirements of BA-triggered cell death because we had previously analyzed the mechanism of apoptosis induced by standard cytotoxic drugs, such as Doxo in neuroblastoma cells (3).

Neuroblastoma cells treated with BA displayed typical morphological features of apoptotic cells, with shrinkage, membrane blebbing, and nuclear fragmentation (data not shown). The dose response of BA-induced apoptosis was assessed by flow cytometry staining DNA with propidium iodide (Fig. 1*B*). DNA fragmentation of neuroblastoma cells treated with BA was also found by agarose gel electrophoresis (data not shown). In addition to DNA analysis, apoptosis was also assessed by annexin V staining, leading to similar results (data not shown). To investigate whether or not BA was active against neuroblastoma cells *ex vivo*, we analyzed cell preparations obtained from tumor specimens by FACS analysis using two-color fluorescence to identify apoptosis in tumor cells by anti-GD2 staining (30). Patients' derived neuroblastoma cells rapidly underwent apoptosis even at low concentrations of 0.5 µg/ml BA (Fig. 1*C*). These results suggest that BA could eventually exert potent antitumor activity *in vivo*.

Caspases Mediate BA-induced Apoptosis. To gain insight into the molecular effector pathway(s) of BA-induced apoptosis, we first analyzed whether caspases involved as downstream effectors in various death signaling pathways mediate BA-triggered apoptosis (32, 34). Activation of the CD95 receptor-proximal caspase FLICE and the downstream caspase CPP32 was monitored to assess different components of the caspase cascade. BA caused a strong increase in caspase activity, which peaked at 18 h after addition of BA (Fig. 2*A*). FLICE was cleaved into p18 active subunits upon treatment with BA (Fig. 2*B*). In addition, CPP32 was proteolytically processed, and PARP, one of the known substrates for CPP32 (35), was cleaved to its characteristic M_r 85,000 fragment (Fig. 2*C*). Incubation with zVAD-fmk almost completely abrogated apoptosis following treatment with BA (Fig. 2*D*) and inhibited cleavage of FLICE and PARP (Fig. 2*E*), indicating that caspases were crucially involved in BA-induced apoptosis. To investigate whether or not BA could directly cleave FLICE, an *in vitro* cleavage assay was performed. After incubating *in vitro*-translated ³⁵S-labeled FLICE with BA for 24 h at 4 or 37°C, no cleavage products were detected, demonstrating that BA did not directly cleave FLICE (data not shown), whereas the activated CD95 DISC cleaved FLICE when used in an *in vitro* FLICE assay (12).

BA Induces Apoptosis Independently of the CD95 System. Activation of FLICE has been described in response to CD95 triggering by recruitment of FLICE to the CD95 DISC (12). We previously found that CD95-L was induced upon drug treatment and mediated apoptosis via CD95 triggering (2). We therefore asked whether stimulation of the CD95 system may account for activation of FLICE following treatment with BA. However, BA did not induce CD95-L mRNA as assessed by RT-PCR, whereas Doxo strongly up-regulated CD95-L mRNA and also stimulated FLICE cleavage (Figs. 3A and 2B). Moreover, no up-regulation of the CD95 protein could be detected following incubation with BA (data not shown), whereas up-regulation of CD95 has been reported in response to cytotoxic drugs (36–38). Blockage of CD95 by F(ab')$_2$ anti-APO-1 antibody fragments previously shown to inhibit autocrine/paracrine death in T cells (31) and drug-triggered apoptosis (2) did not inhibit BA-induced cell death, whereas apoptosis following treatment with Doxo, cisplatinum, and VP-16 was markedly reduced (Fig. 3B). Taken together, these findings indicate that BA-mediated apoptosis was independent of CD95-L/receptor interaction.

BA Induces Disturbance of Mitochondrial Function. Mitochondria have recently been implicated in the apoptotic process and in activation of cytoplasmic proteases (17–19). We therefore investigated the effect of BA on mitochondrial function. Treatment of SH-EP cells with BA caused a disruption of the $\Delta\Psi_m$ followed by hyperproduction of ROS (Fig. 4A; Ref. 17). The early loss of mitochondrial potential may reflect a direct effect of BA on mitochondrial function.[5] $\Delta\Psi_m$ collapse and generation of ROS preceded cleavage of caspases, suggesting that mitochondrial events might be involved in activation of caspases. To determine whether ROS generated in mitochondria had a direct local effect on mitochondrial membranes, the amount of intact cardiolipin, a molecule restricted to the inner mitochondrial membrane, was assessed by means of the fluorochrome NAO (17). As shown in Fig. 4B, mitochondrial ROS generation was accompanied by reduced staining with NAO, suggesting that production of ROS caused an immediate damage of the inner mitochondrial membrane. Thus, BA-induced apoptosis seemed to be associated with mitochondrial dysfunction.

Involvement of Bcl-2 Family Proteins and p53 in BA-induced Apoptosis. Bcl-2 and Bcl-x$_L$ have recently been invoked to maintain cell viability by preventing loss of mitochondrial membrane potential (17). Overexpression of Bcl-2 and Bcl-x$_L$ strongly inhibited disruption of $\Delta\Psi_m$ and hyperproduction of ROS (Fig. 5A) and blocked cleavage of FLICE and PARP (Fig. 5B), further supporting the hypothesis that mitochondrial alterations might be involved in activation of caspases. Furthermore, proapoptotic Bcl-2-related proteins, such as Bax and Bcl-x$_S$, were up-regulated after incubation with BA, whereas expression levels of Bcl-2 and Bcl-x$_L$ were unaffected by treatment with BA (Fig. 5C). p53 was previously shown to be involved in the process of drug-induced apoptosis following DNA damage (39) and may act as a direct transcriptional activator of the bax gene (40). However, no accumulation of wild-type p53 protein was detected upon treatment with BA, whereas wild-type p53 protein strongly increased after treatment of SH-EP cells with Doxo (Fig. 5D). These findings indicate that BA-mediated apoptosis and up-regulation of Bax occurred independently of p53 protein in neuroblastoma cells.

BA Bypasses Resistance to CD95- and Doxo-mediated Apoptosis. Because the molecular mechanism of BA-induced death appeared to be different from activation of CD95-L/receptor interaction induced by other conventional cytotoxic agents, we asked whether or not BA could overcome drug resistance of tumor cells. Parental SH-EP cells
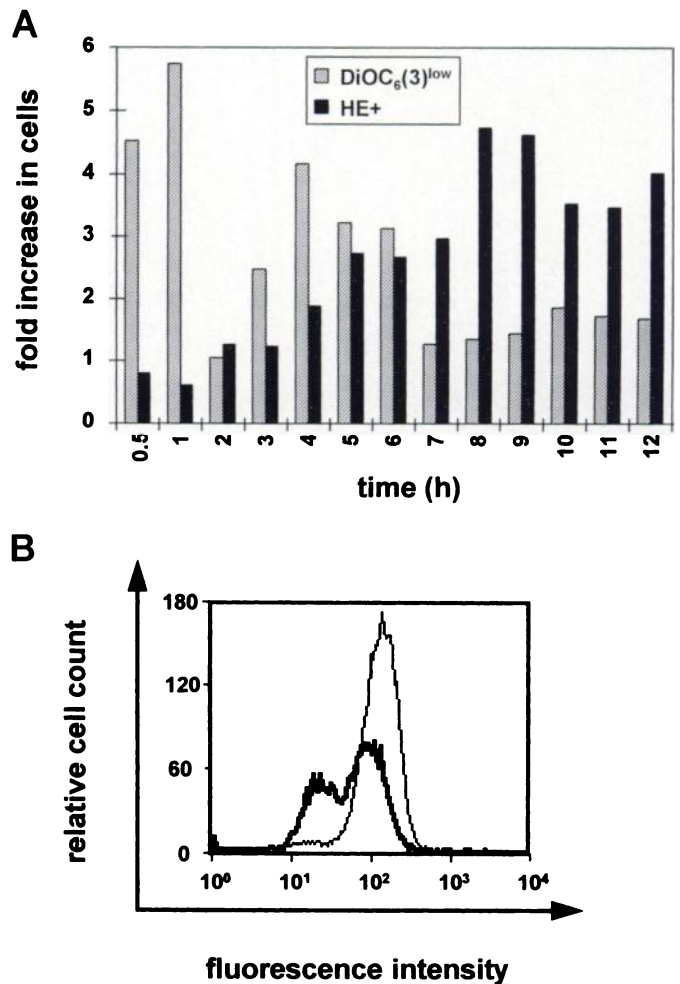
Fig. 4. BA-induced disturbance of mitochondrial function. A, reduction of mitochondrial membrane potential and hyperproduction of ROS. SH-EP neuroblastoma cells were treated with 10 µg/ml BA for the indicated times. Cells were stained with the fluorochrome DiOC$_6$(3) to determine $\Delta\Psi_m$ and with HE to determine ROS generation and analyzed by flow cytometry. Fold increase in cells with low $\Delta\Psi_m$ [DiOC$_6$(3)^{low}] or with enhanced ROS production (HE+) is shown. B, lipid peroxidation. SH-EP neuroblastoma cells treated with 10 µg/ml BA for 24 h (heavy line) or control cells (thin line) were stained with NAO to assess oxidized cardiolipin and analyzed by flow cytometry.

and variant cell lines resistant to anti-CD95 or Doxo were responsive toward BA, whereas anti-CD95- and Doxo-resistant cells were partially resistant to Doxo (Fig. 6A). Moreover, incubation with BA led to cleavage of FLICE and PARP in partially resistant neuroblastoma cells (Fig. 6B). These findings show that BA mediated apoptosis in CD95- and Doxo-resistant SH-EP cells independently of the CD95 system and via activation of caspases. In addition, FLICE and PARP were also processed in other tumor cell lines responsive to BA, such as medulloblastoma (Daoy) and Ewing's sarcoma (A17/95), but not in tumor cells resistant to BA (MCF-7, HT-29, H-146, and KTCTL-26; Fig. 6B).

DISCUSSION

BA has recently been identified as a new antineoplastic agent with specific cytotoxicity against melanoma cells (24). Here, we report that BA was also active on the major solid tumors of childhood, including drug-resistant tumor cells and characterize the molecular requirements for BA-induced apoptosis, which differed from previously identified mechanisms (2).

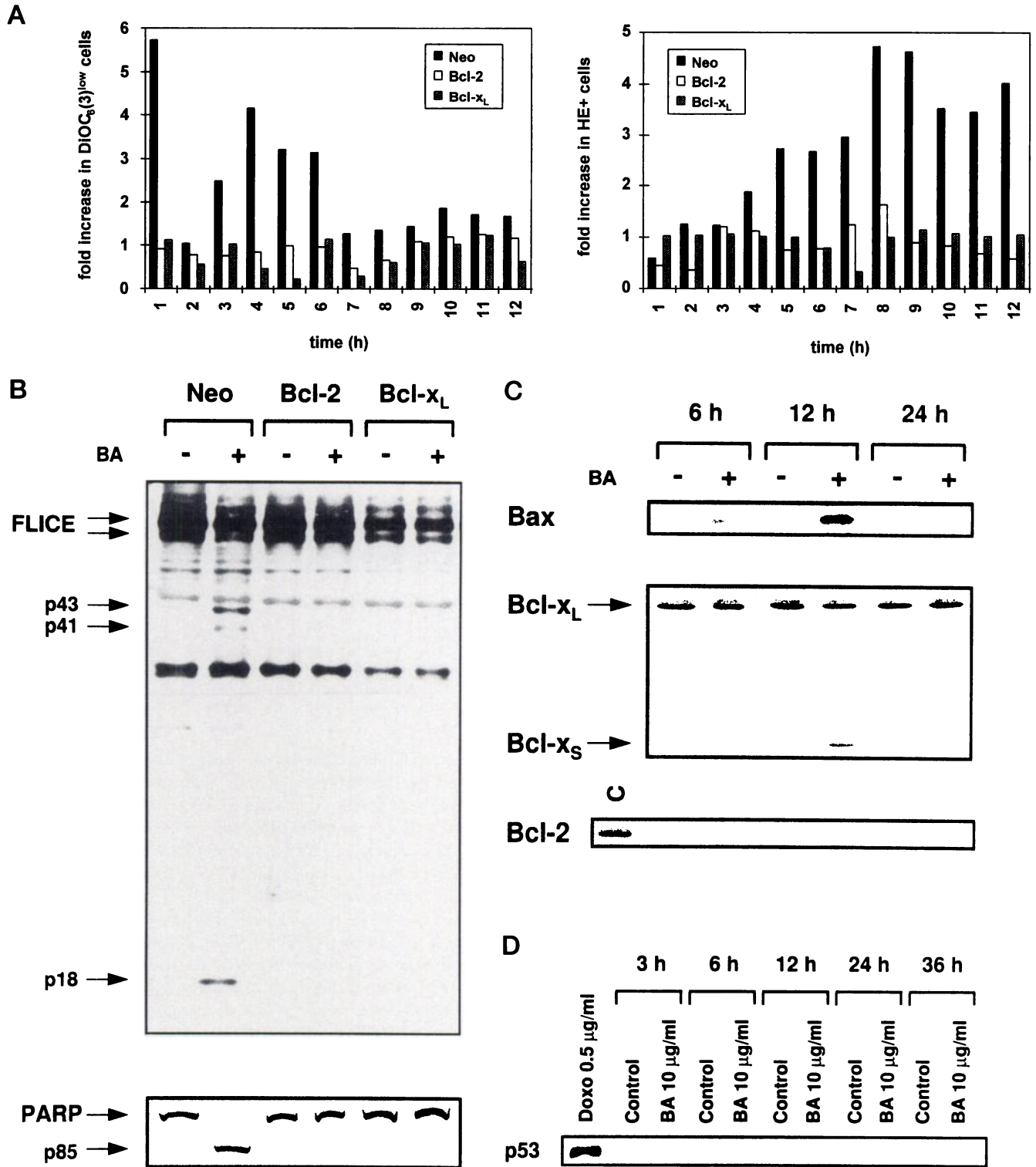BA-triggered apoptosis crucially depended on activation of

Fig. 5. Involvement of Bcl-2 related proteins and p53 in BA-induced apoptosis. *A*, inhibition of BA-induced disturbance of mitochondrial function by overexpression of Bcl-2 and Bcl-x$_L$. SH-EP neuroblastoma cells transfected with a neomycin resistance vector only, bcl-2, or bcl-x$_L$ were treated with 10 μg/ml BA for the indicated times. Cells were stained with the fluorochrome DiOC$_6$(3) to determine ΔΨ$_m$ and with HE to determine ROS generation and analyzed by flow cytometry. Fold increase in cells with low ΔΨ$_m$ [DiOC$_6$(3)^{low} cells, *left panel*] or with enhanced ROS production (HE+ cells, *right panel*) is shown. *B*, inhibition of BA-induced FLICE and PARP cleavage by overexpression of Bcl-2 and Bcl-x$_L$. SH-EP neuroblastoma cells transfected with a neomycin resistance vector only (*Neo*), bcl-2, or bcl-x$_L$ were left untreated (−) or were treated with 10 μg/ml BA for 24 h (+). Western blot analysis for FLICE and PARP cleavage was performed as described in Fig. 2*B*. *C*, induction of Bax and Bcl-x$_S$. SH-EP neuroblastoma cells were treated with 10 μg/ml BA for the indicated times. Forty μg of protein per lane, isolated from cell lysates, were separated by 12% SDS-PAGE. Immunodetection of Bax, Bcl-x, and Bcl-2 was performed by rabbit anti-Bax polyclonal antibody, rabbit anti-Bcl-x polyclonal antibody, and mouse anti-Bcl-2 monoclonal antibody using ECL. Untreated KM3 cells were used as positive control for Bcl-2 expression (*C*). *D*, lack of p53 accumulation during BA-induced apoptosis. SH-EP neuroblastoma cells were treated with 10 μg/ml BA for indicated times or 0.5 μg/ml Doxo for 12 h. Forty μg of protein per lane, isolated from cell lysates, were separated by 12% SDS-PAGE. Immunodetection of p53 was performed by mouse anti-p53 monoclonal antibody using ECL.
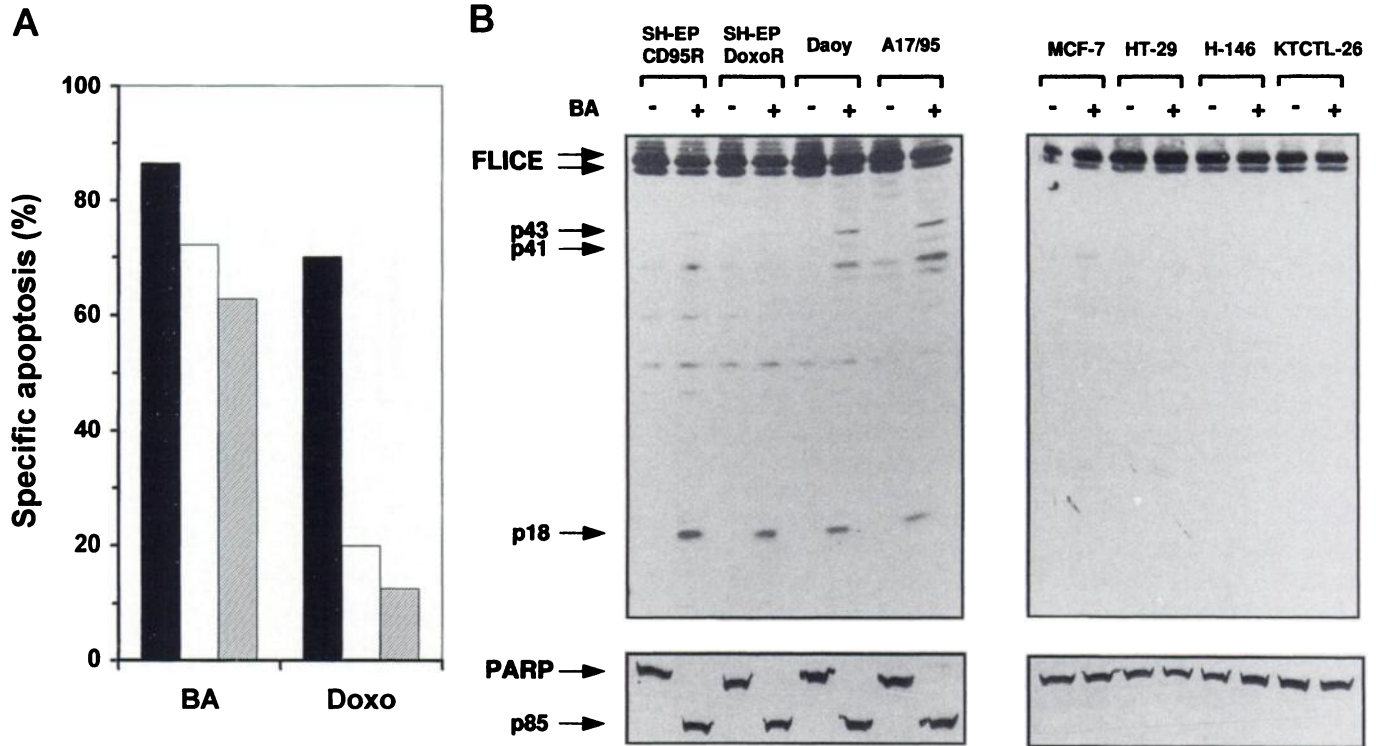
Fig. 6. BA bypasses drug resistance to CD95- and Doxo-mediated apoptosis. *A*, induction of apoptosis by BA in CD95- and Doxo-resistant neuroblastoma cells. SH-EP neuroblastoma cells (■), CD95-resistant SH-EP^{CD95R} cells (□), or Doxo-resistant SH-EP^{DoxoR} cells (▨) were treated with 10 μg/ml BA or 0.5 μg/ml Doxo for 72 h. Specific apoptosis was determined and calculated as described in the legend to Fig. 1*A*. Columns, mean from three independent experiments in triplicate. SDs were less than 10%. *B*, cleavage of FLICE and PARP in BA-sensitive cells. Cells [CD95-resistant neuroblastoma (*SH-EP^{CD95R}*), Doxo-resistant neuroblastoma (*SH-EP^{DoxoR}*), medulloblastoma (*Daoy*), Ewing's sarcoma (*A17/95*), breast carcinoma (*MCF-7*), colon carcinoma (*HT-29*), small cell lung carcinoma (*H-146*), and renal cell carcinoma cells (*KTCTL-26*)] were left untreated (−) or were treated with 10 μg/ml BA for 24 h (+). Forty μg of protein per lane, isolated from cell lysates, were separated by 12% SDS-PAGE. Western blot analysis for FLICE and PARP cleavage was performed as described in the legend to Fig. 2*B*.

caspases because it was blocked by the broad-range peptide inhibitor of caspases zVAD-fmk. Upon incubation of tumor cells with BA, caspase activity increased, and FLICE and CPP32 were enzymatically processed, leading to cleavage of PARP. We previously found that drug-induced apoptosis involved induction of CD95-L expression that mediated cell death via activation of caspases (2, 3). However, upon treatment with BA, stimulation of the CD95 system did not appear to account for activation of caspases because BA did not induce CD95-L, and interference with CD95-L/receptor interaction by blockage of CD95 did not inhibit BA-induced apoptosis. Although other members of the TNF/nerve growth factor family of ligands, such as TNF-α and TRAIL, have also been described to activate caspases following interaction with their cellular receptor (41, 42), they were not found to mediate BA-induced apoptosis (data not shown). Thus, BA-induced activation of caspases and cell death seemed to circumvent ligand/receptor-triggered apoptosis. FLICE has recently been described to be physiologically activated at the CD95 DISC (12). In this study, we identified a novel mechanism of FLICE activation by the cytotoxic drug BA that led to activation of FLICE independent of CD95 triggering. FLICE located upstream in the apoptosis pathway (12), the downstream caspase CPP32, and PARP were almost simultaneously cleaved following BA treatment (Fig. 2 and data not shown), suggesting that these molecules were proteolytically processed in a nonhierarchical manner independent of death receptor triggering. BA appeared to more directly activate FLICE and CPP32, although it did not directly induce autocatalytic cleavage of purified FLICE *in vitro*. However, BA might trigger intracellular events that were upstream or close to the activation of caspases.

Recent data suggest that mitochondria may play a major role in apoptosis (17–19). BA caused an early loss of mitochondrial mem-

brane potential followed by hyperproduction of ROS and oxidation of mitochondrial membrane components, indicating local damage. During BA-induced apoptosis, changes in mitochondrial function clearly preceded activation of both FLICE and CPP32 and nuclear fragmentation. Furthermore, overexpression of Bcl-2 conferred protection against BA-induced apoptosis by blocking dissipation of $\Delta\Psi_m$ and subsequent cleavage of FLICE and PARP, suggesting that mitochondrial alterations might be involved in activation of the caspases tested. Thus, in BA-mediated apoptosis, both FLICE and CPP32 appeared to act downstream of mitochondria, although the relationship between mitochondrial perturbations and activation of proteases in BA-mediated apoptosis remains as yet elusive. Proapoptotic proteins of the Bcl-2 family, such as Bax and Bcl-x$_S$, increased upon BA treatment. Because overexpression of Bax has recently been shown to initiate cell death by activation of caspases and alteration in mitochondrial function (43), Bax might be involved in induction of mitochondrial dysfunction and activation of caspases following treatment with BA.

Wild-type p53 is considered to participate in programmed cell death in response to DNA damage in many tumor cells (39) and has also been reported as a direct transcriptional activator of the human *Bax* gene (40), suggesting that p53 may be responsible for activation of conserved apoptosis pathways. However, no accumulation of wild-type p53 protein was found upon treatment with BA in neuroblastoma cells, although p53 protein accumulated in these cells in response to other cytotoxic drugs. In addition, sensitivity or resistance to BA was variably associated with loss of wild-type p53 function because p53-mutant Daoy medulloblastoma cells (44) were sensitive to BA, whereas p53-mutant HT-29 colon carcinoma cells (45) did not respond to BA. p53-independent death mechanisms after administration of chemotherapeutic drugs or γ-irradiation have been described (46),

and Bax-accelerated apoptosis in response to dexamethasone has been observed in the absence of p53 (47). These data suggest that in addition to p53-restricted pathways, alternative pathways are involved in up-regulation of Bax expression and drug-induced apoptosis.

Our findings may have implications for overcoming drug resistance of tumor cells. CD95- and Doxo-resistant neuroblastoma cells were still responsive to BA, suggesting that drug resistance can be bypassed by activating death signaling pathways downstream of CD95-L/receptor interaction. BA might therefore be a promising new drug for some neuroblastoma patients resistant to standard chemotherapy. BA is an especially attractive new compound because of its significant cytotoxic activity together with its lack of toxicity, leading to a favorable therapeutic index (24, 48–50).

In summary, we identified BA as a cytotoxic agent active against neuroectodermal tumor cells, such as cells from neuroblastoma, medulloblastoma, and Ewing's sarcoma, the most frequent solid tumors of childhood. At present, it is unclear what determined the specificity of BA for neuroectodermal tumors. BA triggered apoptosis signaling pathways distinct from those described previously for standard chemotherapeutic agents. BA induced apoptosis via activation of caspases, probably by interference with mitochondrial function but independently of CD95-L/receptor interaction and wild-type p53 protein. Because BA induced apoptosis even in neuroblastoma cells resistant to conventional cytotoxic drugs, treatment with BA may overcome some forms of drug resistance. In a more general sense, our findings provide new insights into death signaling pathways of drug-sensitive and drug-resistant tumor cells and may lead to the generation of new compounds to target drug resistance of tumor cells. BA seems to be a promising new agent for the treatment of neuroectodermal tumors, such as neuroblastoma, and it clearly warrants further preclinical and clinical evaluation.

ACKNOWLEDGMENTS

REFERENCES

1. Fisher, D. E. Apoptosis in cancer therapy: crossing the threshold. Cell, 78: 539–542, 1994.
2. Friesen, C., Herr, I., Krammer, P. H., and Debatin, K-M. Involvement of the CD95 (APO-1/Fas) receptor/ligand system in drug-induced apoptosis in leukemia cells. Nat. Med., 2: 574–577, 1996.
3. Fulda, S., Sieverts, H., Friesen, C., Herr, I., and Debatin, K. M. The CD95 (APO-1/Fas) system mediates drug-induced apoptosis in neuroblastoma cells. Cancer Res., 57: 3823–3829, 1997.
4. Oehm, A., Behrmann, I., Falk, W., Pawlita, M., Maier, G., Klas, C., Li-Weber, M., Richards, S., Dhein, J., Trauth, B. C., Ponstingl, H., and Krammer, P. H. Purification and molecular cloning of the APO-1 cell surface antigen, a member of the tumor necrosis factor/nerve growth factor receptor superfamily. J. Biol. Chem., 267: 10709–10715, 1992.
5. Leithäuser, F., Dhein, J., Mechtersheimer, G., Koretz, K., Brüderlein, S., Henne, C., Schmidt, A., Debatin, K-M., Krammer, P. H., and Möller, P. Constitutive and induced expression of APO-1, a new member of the nerve growth factor/tumor necrosis factor receptor superfamily, in normal and neoplastic cells. Lab. Invest., 69: 415–429, 1993.
6. Debatin, K-M. Disturbances of the CD95 (APO-1/Fas) system in disorders of lymphohaematopoietic cells. Cell Death Differ., 3: 185–189, 1996.
7. Nagata, S. Apoptosis by death factor. Cell, 88: 355–365, 1997.
8. Peter, M. E., Kischkel, F. C., Hellbrandt, S., Chinnaiyan, A. M., Krammer, P. H., and Dixit, V. M. CD95 (APO-1/Fas)-associating signaling proteins. Cell Death Differ., 3: 161–170, 1996.
9. Muzio, M., Chinnaiyan, A. M., Kischkel, F. C., O'Rourke, K., Shevchenko, A., Ni, J., Scaffidi, C., Bretz, J. D., Zhang, M., Gentz, R., Mann, M., Krammer, P. H., Peter, M. E., and Dixit, V. M. FLICE, a novel FADD-homologous ICE/CED-3-like protease, is recruited to the CD95 (Fas/APO-1) death-inducing signaling complex. Cell, 85: 817–827, 1996.
10. Boldin, M. P., Goncharov, T. M., Goltsev, Y. V., and Wallach, D. Involvement of

MACH, a novel MORT-1/FADD-interacting protease, in Fas/APO-1-and TNF receptor-induced cell death. Cell, 85: 803–815, 1996.
11. Kischkel, F. C., Hellbrandt, S., Behrmann, I., Germer, M., Pawlita, M., Krammer, P. H., and Peter, M. E. Cytotoxicity-dependent APO-1 (Fas/CD95)-associated proteins (CAP) form a death-inducing signaling complex (DISC) with the receptor. EMBO J., 14: 5579–5588, 1995.
12. Medema, J. P., Scaffidi, C., Kischkel, F. C., Shevchenko, A., Mann, M., Krammer, P. H., and Peter, M. E. FLICE is activated by association with the CD95 death-inducing signaling complex (DISC). EMBO J., 16: 2794–2804, 1997.
13. Srinivasula, S. M., Ahmad, M., Fernandes-Alnemri, T., Liwack, G., and Alnemri, E. S. Molecular ordering of the Fas-apoptotic pathway: the Fas/APO-1 protease Mch5 is a CrmA-inhibitable protease that activates multiple Ced-3/ICE-like cysteine proteases. Proc. Natl. Acad. Sci. USA, 93: 14486–14491, 1996.
14. Muzio, M., Salvesen, G. S., and Dixit, V. M. FLICE induced apoptosis in a cell-free system. J. Biol. Chem., 272: 2952–2956, 1997.
15. Suda, T., Takahashi, T., Golstein, P., and Nagata, S. Molecular cloning and expression of the Fas ligand, a novel member of the tumor necrosis factor family. Cell, 75: 1169–1178, 1993.
16. Tanaka, M., Suda, T., Takahashi, T., and Nagata, S. Expression of the functional soluble form of human Fas ligand in activated lymphocytes. EMBO J., 14: 1129–1135, 1995.
17. Kroemer, G., Zamzami, N., and Susin, S. A. Mitochondrial control of apoptosis. Immunol. Today, 18: 44–51, 1997.
18. Zamzami, N., Susin, S. A., Marchetti, P., Hirsch, T., Gomez-Monterrey, I., Castedo, M., and Kroemer, G. Mitochondrial control of nuclear apoptosis. J. Exp. Med., 183: 1533–1544, 1996.
19. Decaudin, D., Geley, S., Hirsch, T., Castedo, M., Marchetti, P., Macho, A., Kofler, R., and Kroemer, G. Bcl-2 and Bcl-x_L antagonize the mitochondrial dysfunction preceding nuclear apoptosis induced by chemotherapeutic agents. Cancer Res., 57: 62–67, 1997.
20. Yang, E., and Korsmeyer, S. J. Molecular thanatopsis: a discourse on the BCL2 family and cell death. Blood, 88: 386–401, 1996.
21. Minn, A. J., Velez, P., Schendel, S. L., Liang, H., Muchmore, S. W., Fesik, S. W., Fill, M., and Thompson, C. B. Bcl-x_L forms an ion channel in synthetic lipid membranes. Nature (Lond.), 385: 353–357, 1997.
22. Schendel, S. L., Xie, Z., Montal, M. O., Matsuyama, S., Montal, M., and Reed, J. C. Channel formation by antiapoptotic protein Bcl-2. Proc. Natl. Acad. Sci. USA, 94: 5113–5118, 1997.
23. Berthold, F., Burdach, S., Kremens, B., Lampert, F., Niethammer, D., Riehm, H., Ritter, J., Treuner, J., Utsch, S., and Zieschang, J. The role of chemotherapy in the treatment of children with neuroblastoma stage IV: the GPO (German Pediatric Oncology Society experience). Klin. Paediatr., 202: 262–269, 1990.
24. Pisha, E., Chai, H., Lee, I. S, Chagwedera, T. E., Farnsworth, N. R., Cordell, G. A., Beecher, C. W., Fong, H. H., Kinghorn, A. D., Brown, D. M., Wani, M. C., Wall, M. E., Hieken, T. J., Das Gupta, T. K., and Pezzuto, J. M. Discovery of betulinic acid as a selective inhibitor of human melanoma that functions by induction of apoptosis. Nat. Med., 1: 1046–1051, 1995.
25. Dole, M., Nuñez, G., Merchant, A. K., Maybaum, J., Rode, C. K., Bloch, C. A., and Castle, V. P. Bcl-2 inhibits chemotherapy-induced apoptosis in neuroblastoma. Cancer Res., 54: 3253–3259, 1994.
26. Dole, M. G., Jasty, R., Cooper, M. J., Thompson, C. B., Nuñez, G., and Castle, V. P. Bcl-x_L is expressed in neuroblastoma cells and modulates chemotherapy-induced apoptosis. Cancer Res., 55: 2576–2582, 1995.
27. Trauth, B. C., Klas, C., Peter, A. M. J., Matz, S., Möller, P., Falk, W., Debatin, K-M., and Krammer, P. H. Monoclonal antibody-mediated tumor regression by induction of apoptosis. Science (Washington DC), 245: 301–305, 1989.
28. Nicoletti, I., Migliorati, G., Pagliacci, M. C., Grignani, F., and Riccardi, C. A rapid and simple method for measuring thymocyte apoptosis by propidium iodide staining and flow cytometry. J. Immunol. Methods, 139: 271–279, 1991.
29. Koopman, G., Reutelingsperger, C. P. M., Kuijten, G. A. M., Keehnen, R. M. J., Pals, S. T., and van Oers, M. H. J. Annexin V for flow cytometric detection of phosphatidylserine expression on B cells undergoing apoptosis. Blood, 84: 1415–1420, 1994.
30. Wu, Z., Schwartz, E., Seeger, R., and Ladisch, S. Expression of GD2 ganglioside by untreated primary human neuroblastomas. Cancer Res., 46: 440–443, 1986.
31. Dhein, J., Walczak, H., Bäumler, C., Debatin, K-M., and Krammer, P. H. Autocrine T-cell suicide mediated by APO-1 (Fas/CD95). Nature (Lond.), 373: 438–441, 1995.
32. Los, M., Van de Craen, M., Penning, L. C., Schenk, H., Westendorp, M., Baeuerle, P. A., Droege, W., Krammer, P. H., Fiers, W., and Schulze-Osthoff, K. Requirement of an ICE/Ced-3 protease for Fas/APO-1-mediated apoptosis. Nature (Lond.), 375: 81–83, 1995.
33. Herr, I., Balemans, L., Böhler, T., Walczak, H., and Debatin, K-M. Monitoring of CD95 (APO-1/Fas) ligand expression in human T-cells by quantitative RT-PCR. Cell Death Differ., 3: 299–305, 1996.
34. Schulze-Osthoff, K., Bauer, M. K. A., Vogt, M., and Los, M. Role of ICE-related and other proteases in Fas-mediated apoptosis. Cell Death Differ., 3: 177–184, 1996.
35. Tewari, M., Quan, L. T., O'Rourke, K., Desnoyers, S., Zeng, Z., Beidler, D. R., Poirier, G. G., Salvesen, G. S., and Dixit, V. M. Yama/CPP32β, a mammalian homolog of Ced-3, is a CrmA-inhibitable protease that cleaves the death substrate poly(ADP-ribose) polymerase. Cell, 81: 801–809, 1995.
36. Debatin, K-M. Anticancer drugs, programmed cell death and the immune system: defining new roles in an old play. J. Natl. Cancer Inst., 89: 750–751, 1997.
37. Micheau, O., Solary, E., Hammann, A., Martin, F., and Dimanche-Boitrel, M-T. Sensitization of cancer cells treated with cytotoxic drugs to Fas mediated cytotoxicity. J. Natl. Cancer Inst., 89: 783–789, 1997.
38. Müller, M., Strand, S., Hug, H., Heinemann, E-M., Walczak, H., Hofmann, W. J., Stremmel, W., Krammer, P. H., and Galle, P. R. Drug-induced apoptosis in hepatoma

cells is mediated by the CD95 (APO-1/Fas) receptor/ligand system and involves activation of wild-type p53. J. Clin. Invest., *99:* 403–413, 1997.

39. Lowe, S. W., Bodis, S., McClatchey, A., Remington, L., Ruley, H. E., Fisher, D. E., Housman, D. E., and Jacks, T. p53 status and the efficacy of cancer therapy *in vivo*. Science (Washington DC), *266:* 807–810, 1994.

40. Miyashita, T., and Reed, J. C. Tumor suppressor p53 is a direct transcriptional activator of the human *bax* gene. Cell, *80:* 293–299, 1995.

41. Marsters, S. A., Pitti, R. M., Donahue, C. J., Ruppert, S., Bauer, K. D., and Ashkenazi, A. Activation of apoptosis by APO-2 ligand is independent of FADD but blocked by CrmA. Curr. Biol., *6:* 750–752, 1996.

42. Higuchi, M., Aggarwal, B. B., and Yeh, E. T. H. Activation of CPP32-like protease in tumor necrosis factor-induced apoptosis is dependent on mitochondrial function. J. Clin. Invest., *99:* 1751–1758, 1997.

43. Xiang, J., Chao, D. T., and Korsmeyer, S. J. Bax-induced cell death may not require interleukin 1β-converting enzyme-like proteases. Proc. Natl. Acad. Sci. USA, *93:* 14559–14563, 1996.

44. Friedman, H. S., Oakes, W. J., Bigner, S. H., Wikstrand, C. J., and Bigner, D. D. Medulloblastoma: tumor biological and clinical perspectives. J. Neuro-oncol., *11:* 1–15, 1991.

45. Wang, Q., Fan, S., Eastman, A., Worland, P. J., Sausville, E. A., and O'Connor, P. M. UCN-01: a potent abrogator of G_2 checkpoint in cancer cells with disrupted p53. J. Natl. Cancer Inst., *88:* 956–965, 1996.

46. Liebermann, D. A., Hoffman, B., and Steinman, R. A. Molecular controls of growth arrest and apoptosis: p53-dependent and independent pathways. Oncogene, *11:* 199–210, 1995.

47. Brady, H. J., Salomons, G. S., Bobeldijk, R. C., and Berns, A. J. T cells from bax-α transgenic mice show accelerated apoptosis in response to stimuli but do not show restored DNA damage-induced cell death in the absence of p53. EMBO J., *15:* 1221–1230, 1996.

48. Sheth, K., Jolad, S., Wiedhopf, R., and Cole, J. R. Tumor-inhibitory agents from *Hyptis emoryi* (Labiatae). J. Pharm. Sci., *61:* 1819, 1972.

49. Miles, D. H., Kokpol, U., Zalkow, L. H., Steindell, S. J., and Nabors, J. B. Tumor inhibitors I: preliminary investigation of antitumor activity of *Sarracenia flava*. J. Pharm. Sci., *63:* 613–615, 1974.

50. Sandberg, F., Dutschewska, H., Christov, V., and Spassov, S. *Spondiathus preussii* var. *glaber* Engler. Pharmaceutic screening of triterpenes. Acta Pharm. Suec., *24:* 253–256, 1987.